Domain bistability in photoexcited GaAs multiple quantum wells

A. M. Tomlinson
Department of Physics, University of Oxford, Clarendon Laboratory, Parks Road, Oxford OX1 3PU, United Kingdom

A. M. Fox
Department of Physics and Astronomy, University of Sheffield, Hicks Building, Sheffield S3 7RH, United Kingdom

C. T. Foxon
Department of Physics, University of Nottingham, University Park, Nottingham NG7 2RD, United Kingdom
(Received 3 August 1999)

We report optical studies of stable electric-field domains in an undoped GaAs multiple-quantum-well *p-i-n* diode. Discontinuities and bistability due to jumps in the domain-wall position were observed in the photocurrent current-voltage characteristic. Simultaneous photoluminescence (PL) measurements confirm the presence of stable domains, and show that the bistability relates to the path history of the domain-wall location. From the PL measurements we have been able to calibrate the field strengths within the domains and determine the sheet charge density in the domain wall.

I. INTRODUCTION

Electric-field domains in semiconductor devices are caused by negative differential resistance (NDR) in the current-voltage characteristic. This can produce a space charge at localized positions within the device, leading to the formation of regions of differing field strengths. Domains were first observed in connection with the Gunn effect in bulk semiconductors, and the concepts were later extended to quantum-well structures in 1974.[1] Since then, there have been many studies of domain effects in quantum wells in a wide range of experimental conditions.[2]

In quantum-well structures, the NDR needed for domain formation is associated with resonant tunneling between confined states in adjacent wells. The field domains are separated from each other by a domain wall located in one of the wells. This quantum well contains the space charge required to maintain the field discontinuity at the boundary. The location of the domain wall is determined by the applied bias, the charge density, and by the detailed form of the current-voltage (I-V) characteristic. This position can be either stable or unstable. In the case of stable domains, discontinuities are observed in the I-V characteristic as the domain-wall jumps from one well to the next on increasing the voltage.[3] Unstable domains, by contrast, do not necessarily lead to I-V discontinuities, but can give rise to self-oscillations[4] and ac-driven chaos.[5]

In this paper, we present optical studies of stable domains in a photoexcited GaAs/$Al_xGa_{1-x}As$ multiple-quantum-well (MQW) structure. The domains manifest themselves by discontinuities in the photocurrent I-V characteristic and by a splitting of the photoluminescence (PL) spectra into well-defined peaks associated with the different domains. This has allowed us to observe domain-related bistability in the I-V curve of a photoexcited MQW device. Previous observations of domain bistability have been restricted to doped MQW devices with electrical injection,[6,7] while bistability due to an optically generated space charge has so far only been observed in single-well structures.[8] Photoinjection has the advantage that it permits the independent control of the bias and carrier density, and also allows monitoring of the domain structure via PL spectroscopy. This allows the position of the domain wall and the magnitude of the space charge to be measured, and permits an unambiguous determination of the domain structure.

II. SAMPLE DESCRIPTION AND EXPERIMENTAL DETAILS

The MQW device was grown by molecular-beam epitaxy on an n^+ GaAs substrate. 25 undoped GaAs/$Al_{0.33}Ga_{0.67}As$ coupled-quantum-well (CQW) units were grown in the intrinsic region of a *p-i-n* structure. The individual CQW units consisted of a 57-Å narrow well and a 158-Å-wide well separated by a 17-Å $Al_{0.33}Ga_{0.67}As$ barrier. Adjacent CQW units were separated from each other by a 153-Å $Al_{0.33}Ga_{0.67}As$ barrier. Tunneling through the thin barrier in the CQW is much faster than the other important time scales in the experiment, so that we can regard the CQW as a single-quantum-well unit in all aspects of the discussion to follow. The sample was chosen because the spatially indirect nature of the electron-hole recombination leads to long radiative lifetimes, making it possible to observe tunneling resonances through the thick barriers separating the CQW units. This gives particularly clear resonant-tunneling peaks in the photocurrent I-V response. Similar results were obtained in another CQW sample with a 79-Å narrow well, and are not discussed further here.

Intrinsic $Al_{0.33}Ga_{0.67}As$ spacer layers of thickness 746 Å were grown between the CQW's and the p and n regions, giving a total i-region thickness of 1.09 μm. The residual doping density of the i region was below the detection limit of our capacitance-voltage profiling setup ($10^{15}\,cm^{-3}$). The p region was 0.75 μm thick and doped at $1.3\times10^{-18}\,cm^{-3}$, with a 0.1-$\mu$m-thick p^+ GaAs capping layer on top. The n region consisted of a 0.24-μm-thick short-period GaAs/AlAs superlattice on top of a 1-μm-thick $Al_{0.67}Ga_{0.33}As$ etch stop and a 0.35-μm-thick GaAs buffer layer. The doping density

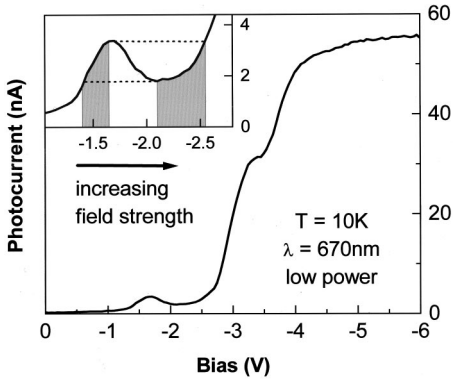

FIG. 1. Photocurrent I-V curve at 10 K using low power excitation at 670 nm. The inset shows the resonant tunneling peak at -1.7 V in more detail. The dashed lines in the inset indicate the limiting conditions in which current continuity can be achieved for two different values of the applied field, as required for the formation of stable domains. The regions of the I-V curve over which this condition can be satisfied are indicated by the shaded areas.

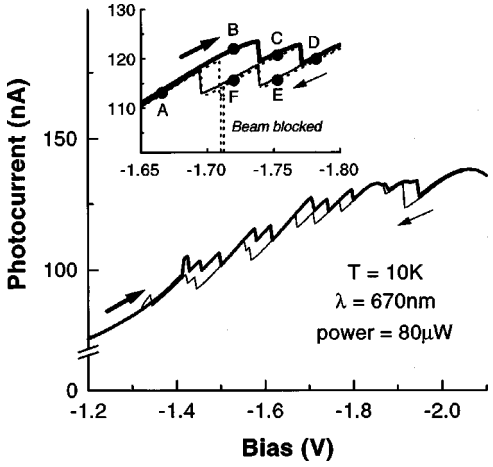

FIG. 2. Photocurrent I-V curves at 80 μW. The thick solid lines correspond to an upsweep (i.e., increasing reverse bias), while the thin solid lines are for a downsweep. The inset shows the bistability between -1.65 and -1.80 V in more detail. The upsweep follows the path *ABCD*, while the downsweep follows path *DEFA*. The dotted lines show the effect of momentarily blocking the light beam during voltage sweeps in both directions.

was $3\times10^{18}\,\mathrm{cm}^{-3}$ in the superlattice, $1.3\times10^{18}\,\mathrm{cm}^{-3}$ in the etch stop, and $3\times10^{18}\,\mathrm{cm}^{-3}$ in the buffer layer. The wafer was selectively etched to produce 400-μm diameter mesas with gold contact pads on each mesa.

The samples were mounted in a helium flow cryostat with optical and electrical access to allow photocurrent measurements at 10 K. Carriers were photoexcited directly into the quantum wells with a diode laser operating at 670 nm. The photocurrent I-V curves were recorded using a Keithley 236 source-measure unit operating in source voltage mode. Simultaneous PL measurements were made using a 0.2-m spectrograph and a Peltier-cooled silicon array detector.

III. RESULTS AND DISCUSSION

Figure 1 shows the photocurrent I-V characteristic of the device measured at low excitation powers. In this context, ''low'' power refers to conditions below the threshold for domain formation, where the shape of the photocurrent I-V curve is independent of the optical power on the sample. Previous photocurrent measurements on this device and similar structures have determined that the vertical transport is governed by the tunneling through the 153-Å barrier that separates the CQW units.[9,10] The general increase of the photocurrent with bias up to the saturation level where all the photoexcited carriers are swept out is caused by nonresonant tunneling and the increase of the electron-hole recombination time. The peaks and shoulders above this general trend are caused by sequential resonant tunneling.

In this paper we concentrate on the NDR associated with the resonant-tunneling peak at -1.7 V, which has a peak-to-valley ratio of ~2, as shown more clearly in the inset to Fig. 1. This resonance corresponds to alignment of the ground state of one CQW unit with the third excited state of the adjacent one.[11] The observed NDR means that the current can be the same for two different field values. The regions of the I-V curve where this is possible are shaded. This allows the field profile across the sample to break into two domain regions while preserving current continuity.

Figure 2 shows the I-V curve recorded when sweeping through the resonant-tunneling peak at -1.7 V when the optical power incident on the sample has been increased by a factor of ~100 to 80 μW. We observe that the increase in the optical power causes fine structure to develop in the I-V curve. The trace shows discontinuities, which is a characteristic signature of the presence of the domains.[12] These discontinuities are caused by discrete jumps of the domain boundary from one CQW unit to the next. Furthermore, on sweeping the voltage in opposite directions, hysteresis is clearly evident in the data. While discontinuities in the I-V curve have been observed in other studies of photoexcited domains,[12] hysteresis has only been observed previously in doped structures.[6,7] Up to 11 jumps are observed in the I-V curve, which is significantly less than the total number of quantum wells in the structure. This reduction in the expected number of domain jumps has been attributed to the influence of the holes.[2] The fact that discontinuities and hysteresis are observed indicates that the domains are stable. This was checked by examining the frequency spectrum of the photocurrent using a spectrum analyzer. No current self-oscillations were observed, in contrast to results obtained in a weakly coupled superlattice device.[13] Additional evidence for the stability of the domains comes from the PL data discussed below.

The inset to Fig. 2 shows the bistability in the I-V curve in more detail near one of the domain-wall jumps. During an upsweep (i.e., on increasing the bias from -1.65 to -1.80 V), the I-V curve follows the path *ABCD*, with domain jumps at -1.74 and -1.77 V. On sweeping the voltage in the opposite direction, the path *DEFA* is followed, with jumps at -1.74 and -1.69 V. The hysteresis in the I-V curve is clearly evident with two open bistable loops. At some other power levels it was possible to obtain three stable values of the photocurrent for a particular voltage. We found that whenever the light beam was temporarily blocked at a voltage in one of the bistable loops, the device returned to the low current state when the beam was unblocked. The dotted lines in the inset to Fig. 2 show this effect. During an

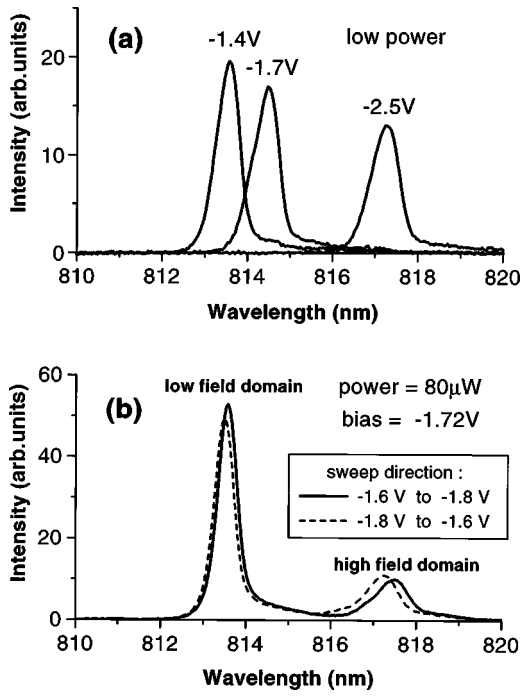

FIG. 3. Photoluminescence recorded (a) at low excitation power and (b) at an optical power level of 80 μW. Spectra for three voltages are shown in (a). In (b) the bias was fixed at -1.72 V, and the two spectra were recorded by sweeping the voltage to -1.72 V in opposite directions. The solid and broken curves correspond to the bistable states represented by points *B* and *F*, respectively, in the inset to Fig. 2.

upsweep, the device starts on the *AB* path, but after blocking the beam at -1.71 V, the current continues along the path *FCD*. On the other hand, if the beam is blocked and unblocked during a downsweep, the state of the device is not altered and the path *DEFA* is mapped out as before. This demonstrates that the device operates as an electro-optic latch. Since the domains are stable, the device will remain on the appropriate current branch until the operating conditions are adjusted to induce a jump to a new branch.

Figure 3 shows the PL spectra obtained from the sample in several different operating conditions. Figure 3(a) shows the PL spectrum obtained at low optical powers when the *I-V* curve takes the form shown in Fig. 1. Three representative voltages are shown. At low powers the charge density inside the depleted diode is negligible and the field across the quantum wells is uniform. The magnitude of this field F is given by

$$F=\frac{V_{\mathrm{bi}}-V_{\mathrm{appl}}}{L_i}, \tag{1}$$

where V_{bi} is the built-in voltage of the diode, V_{appl} is the applied bias, and L_i is the thickness of the i region (1.09 μm). The PL spectrum consists of a single peak centered at the wavelength determined by the quantum confined Stark shift of the ground-state exciton at field strength F. Measurement of the PL peak against applied bias provides a convenient calibration of the field strength experienced by the quantum wells.

Figure 3(b) shows representative PL spectra at an optical power level of 80 μW when the sample exhibits the bistable behavior shown in Fig. 2. In this particular case, the voltage was -1.72 V. The solid line corresponds to arriving at -1.72 V by an upsweep (point *B* in Fig. 2), while the dashed line corresponds to a downsweep (point *F*). In contrast to the low power spectrum at -1.7 V shown in Fig. 3(a), both PL spectra now consist of two well-separated lines. The observation of the two peaks indicates that the field across the quantum wells is not uniform but has broken into two domain regions.[12] The peak that is redshifted compared to the low power spectrum arises from the high field domain, while the blueshifted peak originates from the low field domain. If the optical power was increased further, the PL spectra became more complex, with up to four separate peaks observed due to the presence of more than two domains in the structure. In the work described here, we restrict our attention to power levels where just two peaks are present.

A comparison of Figs. 3(a) and 3(b) allows us to calibrate the field strengths. F_{low} and F_{high}, in the low and high field domains. The PL peak from the low field domain in Fig. 3(b) occurs at approximately the same wavelength as for the Stark-shifted exciton shown in Fig. 3(a) at -1.4 V. This means that the field strengths are the same. If we assume a value of 1.5 V for V_{bi} we can use Eq. (1) to determine that F_{low} is 2.7 V $\mu\mathrm{m}^{-1}$. Similarly, the high field peak is equivalent to a voltage of -2.5 V at low powers, implying that F_{high} is 3.7 V $\mu\mathrm{m}^{-1}$. This calibration allows the size of the low and high field domains (L_{low} and L_{high}, respectively) to be determined according to the relation

$$V_{\mathrm{bi}}-V_{\mathrm{appl}}=F_{\mathrm{low}}L_{\mathrm{low}}+F_{\mathrm{high}}L_{\mathrm{high}}, \tag{2}$$

where we use the fact that $L_{\mathrm{low}}+L_{\mathrm{high}}=L_i=1.09\,\mu$m. With $V_{\mathrm{appl}}=-1.72$ V, we obtain $L_{\mathrm{low}}=0.81\,\mu$m and $L_{\mathrm{high}}=0.28\,\mu$m. This implies that the domain wall is in the vicinity of the 19th quantum well.

The data given in Fig. 3(b) show that both PL peaks are slightly blueshifted for the downsweep direction. This is caused by a small reduction in the field strength in both domains. The magnitude of the blueshift can be calibrated against the Stark shift measured at low carrier densities, thereby enabling us to deduce that F_{low} and F_{high} are reduced by about 0.9% and 1.4%, respectively. This field reduction is consistent with the lower current in the downsweep direction: Fig. 1 shows that both F_{low} and F_{high} must decrease if the current decreases, with a larger decrease in F_{high} due to the smaller gradient of the *I-V* curve. The magnitude of the field change is determined by the requirement of satisfying Eq. (2) with L_{high} increased by one period (0.0385 μm), and L_{low} correspondingly reduced by one period, but with the same value of V_{appl}. The field shifts deduced from the PL data are fully consistent with this condition.

The value obtained above for the size of the domains can be checked against the observed intensity ratios of the two peaks. If there are N wells out of the total of 25 in the low field region, the ratio of the intensities from the two domains will be given by

$$\frac{I_{\mathrm{low}}}{I_{\mathrm{high}}}=\frac{N}{(25-N)}\times\frac{I(F_{\mathrm{low}})}{I(F_{\mathrm{high}})}, \tag{3}$$

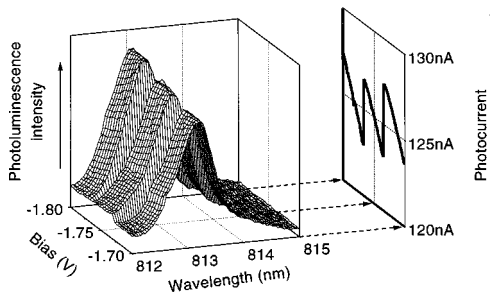

FIG. 4. 3D plot of the photoluminescence peak from the low field domain correlated directly with the discontinuities in the I-V curve during an upsweep from -1.7 to -1.8 V.

where the second factor accounts for the decrease in the PL intensity with increasing field. This value (1.5) can be read directly from the data of Fig. 3(a). The observed intensity ratio of 5.4 on the upsweep implies that $N=19.6$, in excellent agreement with the value obtained from the field calibration. Similarly, the intensity ratio of 4.4 on the downsweep is consistent with a value of $N=18.6$, exactly one less than on the upsweep. The data therefore show clearly that the bistability is caused by the discrete jump of the position of the domain wall by one unit within the MQW structure. The fact that we find noninteger values for N by this method should not be taken as significant: the absolute calibrations are subject to a small fractional error, and the important point is the difference of N by 1 between the two bistable states.

The domain-wall jumps at the discontinuities in the I-V curve can be seen more clearly in the PL data shown in Fig. 4. This shows the PL data recorded from the low field domain as the bias is increased from -1.70 to -1.80 V, with the corresponding I-V curve shown at the side of the PL data. Discrete jumps in the PL peak position are observed at precisely the voltages where discontinuities occur in the I-V curve. This is very direct evidence that the discontinuity in the I-V curve is caused by the shift of the domain-wall boundary.

The magnitude of the space charge at the boundary can be deduced by applying Poisson's equation across the domain wall. The field discontinuity ΔF is related to the sheet charge density σ by $\Delta F=\sigma/(\epsilon_r\epsilon_0)$, where ϵ_r is the relative dielectric constant within the structure. Taking the appropriate averaged value of the dielectric constant to be 12.1, the measured field discontinuity of 1.0 V μm^{-1} implies that the sheet charge density is 1.1×10^{-8} C cm^{-2}. This in turn implies that the difference between the electron and hole densities in the domain wall is 6.7×10^{10} cm^{-2}. These measurements in themselves do not determine the polarity of the space charge. We assume that the domain boundary is negatively charged since the NDR is associated with electron tunneling rather than hole tunneling. This implies that the high field domain is adjacent to the n contact and the low field domain to the p layer.[12]

The calibration of the field strength in the two domains from the PL data allows us to relate the domain dynamics to the I-V response curve. As noted above, the low field domain corresponds to a voltage of -1.4 V, and the high field domain to -2.5 V. At these voltages the currents in the low and high field regions must be the same. On the basis of the low power I-V curve, we would expect the high field voltage to be closer to -2.2 V rather than -2.5 V (see the inset to Fig. 1). This small discrepancy may be caused by the nonlinear changes in the I-V curve caused by the increase in the overall carrier density.

IV. CONCLUSIONS

We have studied the electric-field domains formed in a GaAs CQW device by photocurrent and photoluminescence spectroscopy. The combination of the two techniques permits an unambiguous identification of the domain regions and a calibration of the field strengths within the domains. This in turn determines the sheet charge density in the domain wall. The stable nature of the domains has allowed us to observe photocurrent bistability related to domains. The PL data clearly demonstrate that the bistability is caused by differing positions of the domain wall depending on the path history of the device.

ACKNOWLEDGMENTS

This work was supported by the Royal Society and the EPSRC. The sample was grown at Philips Research Laboratories, and was processed at the EPSRC Central III-V Facility at Sheffield University. We would like to thank Tobias Canzler for help in the early stages of the project.

[1] L. Esaki and L. L. Chang, Phys. Rev. Lett. **33**, 495 (1974).
[2] For a review, see H. T. Grahn, in *Semiconductor Superlattices, Growth and Electronic Properties*, edited by H. T. Grahn (World Scientific, Singapore, 1995), p. 205.
[3] H. T. Grahn, R. J. Haug, W. Müller, and K. Ploog, Phys. Rev. Lett. **67**, 1618 (1991).
[4] J. Kastrup, H. T. Grahn, K. Ploog, and R. Merlin, Solid-State Electron. **40**, 157 (1996).
[5] Y. Zhang, J. Kastrup, R. Klann, K. H. Ploog, and H. T. Grahn, Phys. Rev. Lett. **77**, 3001 (1996).
[6] J. Kastrup, H. T. Grahn, K. Ploog, F. Prengel, A. Wacker, and E. Schöll, Appl. Phys. Lett. **65**, 1808 (1994).
[7] Y. Zhang, R. Klann, K. H. Ploog, and H. T. Grahn, Appl. Phys. Lett. **70**, 2825 (1997).
[8] L. R. Wilson, D. J. Mowbray, M. S. Skolnick, V. N. Astratov, D. W. Peggs, G. J. Rees, J. P. R. David, R. Grey, G. Hill, and M. A. Pate, Phys. Rev. B **55**, R16 045 (1997).
[9] R. G. Ispasoiu, A. M. Fox, C. T. Foxon, J. E. Cunningham, and W. Y. Jan, Semicond. Sci. Technol. **9**, 545 (1994).
[10] R. J. Stone, J. G. Michels, S. L. Wong, C. T. Foxon, R. J. Nicholas, and A. M. Fox, Surf. Sci. **361/362**, 192 (1996).
[11] See Ref. 10. The slight shift of the resonance to higher bias in the present sample is caused by small variations in the wafer homogeneity and by differences in the processing techniques.
[12] H. T. Grahn, H. Schneider, and K. von Klitzing, Phys. Rev. B **41**, 2890 (1990).
[13] A. M. Tomlinson, A. M. Fox, J. E. Cunningham, and W. Y. Jan, Appl. Phys. Lett. **75**, 2067 (1999).